ADER SCHEMES FOR SCALAR HYPERBOLIC CONSERVATION LAWS IN THREE SPACE DIMENSIONS

E.F. Toro[1] and V.A. Titarev[2]

[1] Laboratory of Applied Mathematics, Faculty of Engineering,
University of Trento, Trento, Italy,
E-mail: toro@ing.unitn.it,
Web page: http://www.ing.unitn.it/toro

[2] Department of Mathematics, Faculty of Science,
University of Trento, Trento, Italy,
E-mail: titarev@science.unitn.it,
Web page: http://www.science.unitn.it/∼titarev

In this paper we develop non-linear ADER schemes for time-dependent scalar linear and non-linear conservation laws in one, two and three space dimensions. Numerical results of schemes of up to fifth order of accuracy in *both time and space* illustrate that the designed order of accuracy is achieved in all space dimensions for a fixed Courant number and essentially non-oscillatory results are obtained for solutions with discontinuities.

Key words: high-order schemes, weighted essentially non-oscillatory, ADER, generalized Riemann problem, three space dimensions.

1 Introduction

This paper is concerned with the construction of non-linear schemes of the ADER type for time-dependent scalar linear and non-linear conservation laws in one, two and three space dimensions. The ADER approach was first put forward by Toro and collaborators [22], where the idea was illustrated for solving the linear advection equation with constant coefficients. Formulations were given for one, two and three-dimensional *linear* schemes on regular meshes and implementation of *linear* schemes of up to 10^{th} order in space and time for both the one-dimensional and the two-dimensional case were reported. We also mention the work of Schwartzkopff et al. [13], where linear schemes of upto 6^{th} order in space and time were

constructed. These were then applied to acoustic problems and detailed comparison with other schemes was carried out.

The extension of the ADER approach to non-linear problems relies on the solution of the generalised Riemann problem. For non-linear systems, including source terms, this was presented in [23]. Construction of ADER schemes for the Euler equations using this Riemann problem solution has been reported in [17, 24]. For the construction of schemes as applied to non-linear scalar equations see also [16]. Extension of ADER to scalar advection-diffusion-reaction equations in one space dimension is reported in [18], where explicit non-linear schemes of up to 6^{th} order are presented.

As is well known from the theorem of Godunov [5], high-order *linear* schemes will generate spurious oscillations near discontinuities or sharp gradients of the solution. These oscillations pollute the numerical solution and are thus highly undesirable. To avoid generating spurious oscillations, non-linear solution-adaptive schemes must be constructed. It appears as if it was Kolgan [10] who first proposed to supress spurious oscillations by applying the so-called principle of minimal values of derivatives, producing in this manner a non-oscillatory (TVD) Godunov-type scheme of second order spatial accuracy. Further, more well-known, developments are due to van Leer [25, 26]. In multiple space dimensions unsplit second-order non-oscillatory methods were constructed by Kolgan [11], Tiliaeva [15], Colella [4] and many others. Uniformly high-order extensions of these methods are represented by essentially non-oscillatory (ENO) [8, 2] and weighted essentially non-oscillatory (WENO) [12, 7, 1, 9, 14] schemes.

In one space dimension non-linear ADER schemes of up to fifth order of accuracy in time and space have been presented in [22, 17, 24, 16]. These schemes use essentially non-oscillatory (ENO) or weighted essentially non-oscillatory (WENO) reconstruction procedures to control spurious oscillations. In two space dimensions, however, the ADER approach has so far been limited to linear schemes and linear equations only [22, 13] and therefore cannot be used as such for computing discontinuous solutions. However, we are aware of work in progress by Kaeser (private communication) for the two dimensional non-linear scalar case. We also remark that no three-dimensional ADER schemes, either linear or non-linear, have yet been presented.

The motivation of this paper is twofold. Firstly, we carry out the construction of *non-linear* ADER schemes in two and three space dimensions. These schemes generalize linear two-dimensional ADER schemes developed [22, 13]. Secondly, we extend the ADER approach to non-linear scalar conservation laws with reactive-like source terms in two and three space dimensions thus extending non-linear one-dimensional ADER schemes of [17, 24, 16, 18] to multiple space dimensions.

We present numerical examples for schemes of up to fifth order of accuracy in *both time and space*, which illustrate that the schemes indeed retain the designed order of accuracy in all space dimensions, for a *fixed* Courant number, and produce essentially non-oscillatory results for solutions with discontinuities.

The rest of the paper is organized as follows. In Section 2 we review the ADER approach in one space dimension as applied to advection-reaction equations. Extension to two and three space dimensions is carried out in Sections 3 and 4. Numerical results are provided in Section

6 and conclusions are drawn in Section 7.

2 Review of ADER schemes in one space dimension

Consider the following one-dimensional nonlinear advection-reaction equation:

$$\partial_t q + \partial_x f(q) = s(x,t,q), \tag{1}$$

where $q(x,t)$ is the unknown conservative variable, $f(q)$ is the physical flux and $s(x,t,q)$ is a source term. Integration of (1) over the control volume in $x-t$ space $I_i \times \Delta t$, $I_i = [x_{i-1/2}, x_{i+1/2}]$, of dimensions $\Delta x = x_{i+1/2} - x_{i-1/2}$, $\Delta t = t^{n+1} - t^n$, gives

$$q_i^{n+1} = q_i^n + \frac{\Delta t}{\Delta x}\left(f_{i-1/2} - f_{i+1/2}\right) + \Delta t\, s_i, \tag{2}$$

where q_i^n is the cell average of the solution at time level t^n, $f_{i+1/2}$ is the time average of the physical flux at cell interface $x_{i+1/2}$ and s_i is the time-space average of the source term over the control volume:

$$\begin{gathered} q_i^n = \frac{1}{\Delta x}\int_{x_{i-1/2}}^{x_{i+1/2}} q(x,t^n)\,dx, \quad f_{i+1/2} = \frac{1}{\Delta t}\int_{t^n}^{t^{n+1}} f(q(x_{i+1/2},\tau))\,d\tau, \\ s_i = \frac{1}{\Delta t}\frac{1}{\Delta x}\int_{t^n}^{t^{n+1}}\int_{x_{i-1/2}}^{x_{i+1/2}} s(x,\tau,q(x,\tau))\,dx\,d\tau. \end{gathered} \tag{3}$$

Equation (2) involving the integral averages (3) is upto this point an exact relation, but can be used to construct numerical methods to compute approximate solutions to (1). This is done by subdividing the domain of interest into many disjoint control volumes and by defining approximations to the flux integrals, called numerical fluxes, and to the source integral, called numerical source. Let us denote the approximations to these integrals by the same symbols $f_{i+\frac{1}{2}}$ and s_i in (3). Then the formula (2) is a conservative one-step scheme to solve (1).

The ADER approach defines numerical fluxes and numerical sources in such a way that the explicit conservative one-step formula (2) computes numerical solutions to (1) to arbitrarily high order of accuracy in both space and time. The approach consists of three steps: (i) reconstruction of point wise values from cell averages, (ii) solution of a generalized Riemann problem at the cell interface and evaluation of the intercell flux $f_{i+1/2}$, (iii) evaluation of the numerical source term s_i by integrating a time-space Taylor expansion of the solution inside the cell.

The point-wise values of the solution at $t = t^n$ are reconstructed from cell averages by means of high-order polynomials. To avoid spurious oscillations essentially non-oscillatory (ENO) [8] or weighted essentially non-oscillatory (WENO) [12, 7] reconstruction can be used leading to *non-linear* schemes. In general, WENO reconstruction produces more accurate results and therefore it is used in the design of our schemes. By means of the reconstruction step the conservative variable is represented by polynomials $p_i(x)$ in each cell I_i. At each cell interface

we then have the following generalized Riemann problem:

$$\begin{aligned} &\partial_t q + \partial_x f(q) = s(x,t,q), \\ &q(x,0) = \begin{cases} q_L(x) = p_i(x), & x < x_{i+1/2}, \\ q_R(x) = p_{i+1}(x), & x > x_{i+1/2}. \end{cases} \end{aligned} \tag{4}$$

This generalisation of the Riemann problem is twofold: (i) the governing equations include non-linear advection as well as reaction terms and (ii) the initial condition consists of two reconstruction polynomials of $(r-1)^{th}$ order for a scheme of r^{th} order of accuracy. By the order of accuracy we mean the convergence rate of the scheme when the mesh is refined with a *fixed* Courant number.

We find an approximate solution for the interface state $q(x_{i+1/2}, \tau)$, where τ is local time $\tau = t - t^n$, using a semi-analytical method [23]. The method gives the solution at $x = x_{i+1/2}$ at a time τ, assumed to be sufficiently small, in terms of solutions of a sequence of *conventional* Riemann problems for *homogeneous* advection equations. First we write a Taylor expansion of the interface state in time:

$$q(x_{i+1/2}, \tau) = q(x_{i+1/2}, 0+) + \sum_{k=1}^{r-1} \left[\partial_t^{(k)} q(x_{i+1/2}, 0+)\right] \frac{\tau^k}{k!}, \quad \partial_t^{(k)} q(x,t) = \frac{\partial^k}{\partial t^k} q(x,t), \tag{5}$$

where $0+ \equiv \lim_{t \to 0+} t$. The leading term $q(x_{i+1/2}, 0+)$ accounts for the interaction of the boundary extrapolated values $q_L(x_{i+1/2})$ and $q_R(x_{i+1/2})$ and is the self-similar solution of the *conventional* Riemann problem with the piece-wise constant data:

$$\left.\begin{aligned} &\partial_t q + \partial_x f(q) = 0 \\ &q(x,0) = \begin{cases} q_L(x_{i+1/2}) & \text{if} \quad x < x_{i+1/2} \\ q_R(x_{i+1/2}) & \text{if} \quad x > x_{i+1/2} \end{cases} \end{aligned}\right\} \tag{6}$$

evaluated at $(x - x_{i+1/2})/t = 0$. We call $q(x_{i+1/2}, 0+)$ the Godunov state [5]. Next, we replace all time derivatives by space derivatives using equation (1) by means of the Cauchy-Kowalewski procedure. This procedure can be easily carried out with the aid of algebraic manipulators, such as MAPLE or Mathematica. For example, for the model inviscid reactive Burgers' equation

$$q_t + \left(\frac{1}{2} q^2\right)_x = Aq, \quad A = \text{constant}, \tag{7}$$

the Cauchy-Kowalewski procedure yields the following expressions for time derivatives:

$$\begin{aligned} &q_t = -q q_x + Aq, \\ &q_{tt} = 2\, q\, {q_x}^2 - 3\, q_x\, Aq + q^2 q_{xx} + A^2 q \end{aligned} \tag{8}$$

and so on. Expressions (8) contain unknown space derivatives of the solution

$$q^{(k)} \equiv \frac{\partial^k}{\partial x^k} q, \quad q^{(1)} \equiv q_x, \quad q^{(2)} \equiv q_{xx}, \quad q^{(3)} \equiv q_{xxx}, \quad \ldots,$$

at cell interface position $x_{i+1/2}$ and time $\tau = 0$. It can be shown that by differentiating the governing equation with respect to x we can obtain evolution equations for each $q^{(k)}$. Generally, these evolution equations are non-linear and inhomogeneous: for a fixed $k > 0$ the source terms depend on lower order derivatives $q^{(k-1)}$, $q^{(k-2)}$ etc. For each k we then pose a generalized Riemann problem with initial conditions obtained by taking appropriate derivatives of $q_L(x)$, $q_R(x)$ with respect to x; we call these problems *derivative* Riemann problems [22]. Because we only need the Godunov state of these derivative Riemann problems we can replace them by the following *linear*, homogenuous conventional Riemann problem:

$$\begin{gathered}\partial_t q^{(k)} + \lambda_{i+1/2}\partial_x q^{(k)} = 0, \quad \lambda_{i+1/2} = \lambda(q(x_{i+1/2}, 0+)), \\ q^{(k)}(x,0) = \begin{cases} \partial_x^{(k)} q_L(x_{i+1/2}), & x < x_{i+1/2}, \\ \partial_x^{(k)} q_R(x_{i+1/2}), & x > x_{i+1/2}. \end{cases} \\ k = 1, \ldots, r-1\end{gathered} \tag{9}$$

Having found the solution at $x = x_{i+1/2}$ of all these derivative Riemann problems we substitute them into Taylor expansion (5) and obtain an approximate solution $q_{i+1/2}(\tau)$:

$$q_{i+1/2}(\tau) = a_0 + a_1\tau + a_2\tau^2 + \ldots + a_{r-1}\tau^{r-1}, \quad 0 \le \tau \le \Delta t, \quad a_i = \text{constant}, \tag{10}$$

which approximates the interface state $q(x_{i+1/2}, \tau)$ to the r^{th} order of accuracy:

$$q_{i+1/2}(\tau) = q(x_{i+1/2}, \tau) + O(\tau^r), \quad 0 \le \tau \le \Delta t. \tag{11}$$

Two options exist to evaluate the numerical flux. The first option is the **state-expansion** ADER [17], in which an appropriate r^{th}-order accurate Gaussian rule is used to evaluate the numerical flux:

$$\hat{f}_{i+1/2} = \sum_{\alpha=0}^{N} f(q_{i+1/2}(\gamma_\alpha \Delta t)) K_\alpha \tag{12}$$

where γ_j and K_α are properly scaled nodes and weights of the rule and N is the number of nodes.

The second option to evaluate the numerical flux is the **flux-expansion** ADER [24, 16], in which we seek Taylor time expansion of the physical flux at $x_{i+1/2}$

$$f(x_{i+1/2}, \tau) = f(x_{i+1/2}, 0+) + \sum_{k=1}^{r-1} \left[\partial_t^{(k)} f(x_{i+1/2}, 0+)\right] \frac{\tau^k}{k!}. \tag{13}$$

From (13) and the second equation in (3) the numerical flux is now given by

$$f_{i+1/2} = f(x_{i+1/2}, 0+) + \sum_{k=1}^{r-1} \left[\partial_t^{(k)} f(x_{i+1/2}, 0+)\right] \frac{\Delta t^k}{(k+1)!}. \tag{14}$$

The leading term $f(x_{i+1/2}, 0+)$ accounts for the first interaction of left and right boundary extrapolated values and is computed from (6) using a monotone flux, such as Godunov's first

order upwind flux. Following [24], the remaining higher order time derivatives of the flux in (14) are expressed via time derivatives of the intercell state $q_{i+1/2}(\tau)$

$$\frac{\partial}{\partial t}f = \frac{\partial f}{\partial q}\frac{\partial}{\partial t}q, \quad \frac{\partial^2}{\partial t^2}f = \frac{\partial^2 f}{\partial q^2}\left(\frac{\partial}{\partial t}q\right)^2 + \frac{\partial f}{\partial q}\frac{\partial^2}{\partial t^2}q, \tag{15}$$

where from (10)

$$\frac{\partial}{\partial t}q = a_1, \quad \frac{\partial^2}{\partial t^2}q = a_2, \tag{16}$$

and so on. No numerical quadrature is then required to compute the numerical flux.

An improvement of the flux-expansion ADER approach is the so-called ADER-TVD approach [24]. In ADER-TVD schemes the leading term in the flux expansion (14) is computed from (6), not as a first order upwind flux, but as a second order TVD flux with a compressive limiter, such as the flux of the Weighted Average Flux scheme [20, 21].

Now we deal with the treatment of the source term. The first step in the evaluation of the numerical source term s_i^n in (3) is to discretize the space integral by means of a N-point Gaussian rule [18]:

$$s_i = \sum_{\alpha=1}^{N}\left(\frac{1}{\Delta t}\int_{t^n}^{t^{n+1}} s(x_\alpha, \tau, q(x_\alpha, \tau))d\tau\right)K_\alpha, \tag{17}$$

where K_α are the scaled weights of the rule, x_α are the Gaussian integration points and N is the total number of points in the rule.

Next for each Gaussian point x_α (which are different from $x_{i\pm1/2}$) we reconstruct values of q and its space derivatives by means of the WENO reconstruction, write the time Taylor expansion of the form (5) and perform the Cauchy-Kowalewski procedure to replace all time derivatives by space derivatives. As a result we obtain high-order approximations to $q(x_\alpha, \tau)$, $\alpha = 1, \ldots, N$ of the form (10). Finally, the time integration in (17) is carried out by means of a Gaussian quadrature:

$$s_i = \sum_{\alpha=1}^{N}\left(\sum_{l=1}^{N} s(x_\alpha, \tau_l, q(x_\alpha, \tau_l))K_l\right)K_\alpha. \tag{18}$$

The solution is advanced by one time step by updating the cell averages of the solution according to the one-step formula (2).

3 Extension to two space dimensions

Consider the following two-dimensional nonlinear advection-reaction equation:

$$\partial_t q + \partial_x f(q) + \partial_y g(q) = s(x, y, t, q), \tag{19}$$

where $q(x, y, t)$ is the unknown conservative variable, $f(q)$, $g(q)$ are the advection fluxes in x and y coordinate directions respectively and $s(x, y, t, q)$ is a source term. Integration of (19) over the control volume in $x - y - t$ space $I_{ij} \times \Delta t$, with

$$I_{ij} = [x_{i-1/2}, x_{i+1/2}] \times [y_{j-1/2}, y_{j+1/2}],$$

of dimensions $\Delta x = x_{i+1/2} - x_{i-1/2}$, $\Delta y = y_{j+1/2} - y_{j-1/2}$, $\Delta t = t^{n+1} - t^n$, gives

$$q_{ij}^{n+1} = q_{ij}^n + \frac{\Delta t}{\Delta x}\left(f_{i-1/2,j} - f_{i+1/2,j}\right) + \frac{\Delta t}{\Delta y}\left(g_{i,j-1/2} - g_{i,j+1/2}\right) + \Delta t\, s_{ij}\,, \tag{20}$$

where q_{ij}^n, $f_{i+1/2,j}$, $g_{i,j+1/2}$ and s_{ij} are now given by

$$q_{ij}^n = \frac{1}{\Delta x}\frac{1}{\Delta y}\int_{x_{i-1/2}}^{x_{i+1/2}}\int_{y_{j-1/2}}^{y_{j+1/2}} q(x,y,t^n)\,dy\,dx, \tag{21}$$

$$\left.\begin{aligned} f_{i+1/2,j} &= \frac{1}{\Delta t}\frac{1}{\Delta y}\int_{y_{j-1/2}}^{y_{j+1/2}}\int_{t^n}^{t^{n+1}} f(q(x_{i+1/2},y,\tau))\,d\tau\,dy, \\ g_{i,j+1/2} &= \frac{1}{\Delta t}\frac{1}{\Delta x}\int_{x_{i-1/2}}^{x_{i+1/2}}\int_{t^n}^{t^{n+1}} g(q(x,y_{i+1/2},\tau))\,d\tau\,dx, \end{aligned}\right\} \tag{22}$$

$$s_{ij} = \frac{1}{\Delta t}\frac{1}{\Delta x}\frac{1}{\Delta y}\int_{t^n}^{t^{n+1}}\int_{x_{i-1/2}}^{x_{i+1/2}}\int_{y_{j-1/2}}^{y_{j+1/2}} s(x,y,t,q(x,y,t))\,dy\,dx\,dt. \tag{23}$$

The procedure to evaluate the fluxes in two space dimensions consists of three main steps. The first step in evaluating the fluxes is to discretize the spatial integrals over the cell sides in (22) using an r^{th} order Gaussian numerical quadrature. For the rest of this section we shall concentrate on $f_{i+1/2,j}$; the expression for $g_{i,j+1/2}$ is obtained in an entirely analogous manner. The application of a one-dimensional N-point quadrature rule to (22) yields the following expression for the numerical flux in the x coordinate direction:

$$f_{i+1/2,j} = \sum_{\alpha=1}^{N}\left(\frac{1}{\Delta t}\int_{t^n}^{t^{n+1}} f(q(x_{i+1/2},y_\alpha,\tau))d\tau\right)K_\alpha, \tag{24}$$

where $(x_{i+1/2}, y_\alpha)$ are the integration points over the cell side $[y_{j-1/2}, y_{j+1/2}]$ and K_α, K_β are the weights.

The second step in evaluating the fluxes is to reconstruct the point-wise values of the solution from cell averages to high order of accuracy at the Gaussian integration points $(x_{i+1/2}, y_\alpha)$. In this paper we use the so-called dimension-by-dimension reconstruction which is explained in [2, 14] in the context of the two-dimensional ENO and WENO schemes. The reconstruction consists of two one-dimensional WENO reconstruction sweeps. First we perform one-dimensional WENO sweep in the x coordinate direction (normal to the cell interface) and obtain left and right y-averages of q and its x - derivatives. Next we perform the final sweep in y direction and obtain the sought point-wise values of q and its space derivatives.

After the reconstruction is carried out for each point y_α along the cell side $[y_{j-1/2}, y_{j+1/2}]$ we pose the generalized Riemann problem (4) in the x-coordinate direction (normal to the cell boundary) and obtain a high order approximation to $q(x_{i+1/2}, y_\alpha, \tau)$. All steps of the solution procedure remain essentially as before. First, we write the Taylor series expansion in time

$$q(x_{i+1/2},y_\alpha,\tau) = q(x_{i+1/2},y_\alpha,0+) + \sum_{k=1}^{r-1}\left[\partial_t^{(k)} q(x_{i+1/2},y_\alpha,0+)\right]\frac{\tau^k}{k!}. \tag{25}$$

The leading term $q(x_{i+1/2}, y_\alpha, 0+)$ is the self-similar solution of the conventional Riemann problem

$$\left.\begin{aligned} &\partial_t q + \partial_x f(q) = 0, \\ &q(x,0) = \begin{cases} q_L(x_{i+1/2}, y_\alpha) & \text{if} \quad x < x_{i+1/2}, \\ q_R(x_{i+1/2}, y_\alpha) & \text{if} \quad x > x_{i+1/2}. \end{cases} \end{aligned}\right\} \tag{26}$$

evaluated at $(x - x_{i+1/2})/t = 0$. Next, we replace all time derivatives by space derivatives using (19) by means of the Cauchy-Kowalewski procedure, which will now involve not only x derivatives, but also all mixed and y derivatives up to order $r-1$. For example, for the inviscid reactive Burgers' equation

$$q_t + \left(\frac{1}{2}q^2\right)_x + \left(\frac{1}{2}q^2\right)_y = Aq, \quad A = \text{constant}, \tag{27}$$

the Cauchy-Kowalewski procedure yields the following expressions for time derivatives:

$$\begin{aligned} &q_t = -q\,q_x - q\,q_y + Aq, \\ &q_{tt} = 2\,q{q_x}^2 + 4\,q_x\,q q_y - 3\,q_x\,Aq + q^2 q_{xx} + 2\,q^2 q_{xy} + 2\,q{q_y}^2 - 3\,q_y\,Aq + q^2 q_{yy} + A^2 q \end{aligned} \tag{28}$$

and so on. The expressions in (28) contain space derivatives of the solution

$$q^{(k_1,k_2)} \equiv \frac{\partial^{k_1+k_2}}{\partial x^{k_1} \partial y^{k_2}} q, \quad q^{(1,0)} \equiv q_x, \quad q^{(0,1)} \equiv q_y, \quad q^{(1,1)} \equiv q_{xy}, \ldots \tag{29}$$

It can be shown that all $q^{(k_1,k_2)}$ obey inhomogeneous evolution equations, which are obtained by taking spatial derivatives of the governing equation. Similar to the one-dimensional case, since we need only the values at $(x - x_{i+1/2})/t = 0$, all space derivatives can be computed as the Godunov states of the corresponding linear homogeneous derivative Riemann problems:

$$\begin{aligned} &\partial_t q^{(k_1,k_2)} + \lambda_{i+1/2,\alpha}\,\partial_x q^{(k_1,k_2)} = 0, \quad \lambda_{i+1/2,\alpha} = \lambda(q(x_{i+1/2}, y_\alpha, 0+)), \\ &q^{(k_1,k_2)}(x,0) = \begin{cases} \dfrac{\partial^{k_1+k_2}}{\partial x^{k_1} \partial y^{k_2}} q_L(x_{i+1/2}, y_\alpha), & x < x_{i+1/2}, \\ \dfrac{\partial^{k_1+k_2}}{\partial x^{k_1} \partial y^{k_2}} q_R(x_{i+1/2}, y_\alpha), & x > x_{i+1/2}. \end{cases} \end{aligned} \tag{30}$$

Here

$$\frac{\partial^{k_1+k_2}}{\partial x^{k_1} \partial y^{k_2}} q_L(x_{i+1/2}, y_\alpha), \quad \frac{\partial^{k_1+k_2}}{\partial x^{k_1} \partial y^{k_2}} q_R(x_{i+1/2}, y_\alpha)$$

are left and right reconstructed point-wise values of derivatives.

After solving (30) for $1 \le k_1 + k_2 \le r-1$ we substitute $q^{(k_1,k_2)}$ into Taylor expansion (13) and form a polynomial $q_{i+1/2,\alpha}(\tau)$:

$$q_{i+1/2,\alpha}(\tau) = b_0 + b_1\tau + b_2\tau^2 + \ldots + b_{r-1}\tau^{r-1}, \quad 0 \le \tau \le \Delta t, \quad b_i = \text{constant} \tag{31}$$

which approximates the interface state $q(x_{i+1/2}, y_\alpha, \tau)$ at the Gaussian integration point $(x_{i+1/2}, y_\alpha)$ to the r^{th} order of accuracy.

Finally, once approximations to $q(x_{i+1/2}, y_\alpha, \tau)$ for all α are built we can carry out time integration in (24). For the **state-expansion** ADER schemes we use the N-point (r^{th} order accurate) Gaussian quadrature:

$$f_{i+1/2,j} = \sum_{\alpha=1}^{N} \left(\sum_{l=1}^{N} f(q_{i+1/2,\alpha}(\tau_l)) K_l \right) K_\alpha. \tag{32}$$

For the **flux-expansion** ADER schemes we write the Taylor time expansion of the physical flux at each point $x_{i+1/2}$, y_α

$$f(x_{i+1/2}, y_\alpha, \tau) = f(x_{i+1/2}, y_\alpha, 0+) + \sum_{k=1}^{r-1} \left[\partial_t^{(k)} f(x_{i+1/2}, y_\alpha, 0+) \right] \frac{\tau^k}{k!}. \tag{33}$$

Similar to the one-dimensional case, the leading term $f(x_{i+1/2}, y_\alpha, 0+)$ is computed from (26) using a monotone flux, such as Godunov's first order upwind flux. The remaining higher order time derivatives of the flux in (33) are expressed via time derivatives of the intercell state $q_{i+1/2,\alpha}(\tau)$, see (15), (16); the only difference is that now time derivatives of q are given by the time expansion (31). The numerical flux is given by

$$f_{i+1/2,j} = \sum_{\alpha=1}^{N} \left(f(x_{i+1/2}, y_\alpha, 0+) + \sum_{k=1}^{r-1} \left[\partial_t^{(k)} f(x_{i+1/2}, y_\alpha, 0+) \right] \frac{\Delta t^k}{(k+1)!} \right) K_\alpha \,. \tag{34}$$

The computation of the numerical source consists of four steps. First we use the tensor product of the N-point Gaussian rule to discretize the two-dimensional space integral in (23) so that the expression for s_{ij} reads

$$s_{ij} = \sum_{\alpha=1}^{N} \sum_{\beta=1}^{N} \left(\frac{1}{\Delta t} \int_{t^n}^{t^{n+1}} s(x_\alpha, y_\beta, \tau, q(x_\alpha, y_\beta, \tau)) d\tau \right) K_\alpha K_\beta. \tag{35}$$

Then we reconstruct values and all spatial derivatives, including mixed derivatives, of q at the Gaussian integration point in $x-y$ plane for the time level t^n. Note that these points are different from flux integration points along cell sides. The reconstruction procedure is essentially the same as for the flux computation: first we perform reconstruction in the x direction, then in the y direction, or vice versa. Next, for each Gaussian point (x_α, y_β) we perform the Cauchy-Kowalewski procedure and replace time derivatives by space derivatives. As a result we have high-order approximations to $q(x_\alpha, y_\beta, \tau)$, where $\alpha, \beta = 1, \ldots N$. Finally, we carry out numerical integration in time using the Gaussian quadrature:

$$s_{ij} = \sum_{\alpha=1}^{N} \sum_{\beta=1}^{N} \left(\sum_{l=1}^{N} s(x_\alpha, y_\beta, \tau, q(x_\alpha, y_\beta, \tau_l)) K_l \right) K_\beta K_\alpha. \tag{36}$$

The solution is advanced by one time step by updating the cell averages of the solution according to the one-step formula (20).

4 Three space dimensions

Consider the following three-dimensional nonlinear advection-reaction equation:

$$\partial_t q + \partial_x f(q) + \partial_y g(q) + \partial_z h(q) = s(x, y, z, t, q), \tag{37}$$

Integration of (37) over the control volume $I_{ijk} \times \Delta t$, with

$$I_{ijk} = [x_{i-1/2}, x_{i+1/2}] \times [y_{j-1/2}, y_{j+1/2}] \times [z_{k-1/2}, z_{k+1/2}],$$

of dimensions

$$\Delta x = x_{i+1/2} - x_{i-1/2}, \quad \Delta y = y_{j+1/2} - y_{j-1/2}, \quad \Delta z = z_{k+1/2} - z_{k-1/2}, \quad \Delta t = t^{n+1} - t^n$$

gives

$$\begin{aligned} q_{ijk}^{n+1} = q_{ijk}^n \quad &+ \frac{\Delta t}{\Delta x}\left(f_{i-1/2,jk} - f_{i+1/2,jk}\right) + \frac{\Delta t}{\Delta y}\left(g_{i,j-1/2,k} - g_{i,j+1/2,k}\right) \\ &+ \frac{\Delta t}{\Delta z}\left(h_{ij,k-1/2} - h_{ij,k+1/2}\right) + \Delta t\, s_{ijk}, \end{aligned} \tag{38}$$

where q_{ijk}^n, $f_{i+1/2,jk}$, $g_{i,j+1/2,k}$, $h_{ij,k+1/2}$ and s_{ijk} are given by

$$q_{ijk}^n = \frac{1}{\Delta x}\frac{1}{\Delta y}\frac{1}{\Delta z}\int_{x_{i-1/2}}^{x_{i+1/2}}\int_{y_{j-1/2}}^{y_{j+1/2}}\int_{y_{j-1/2}}^{y_{j+1/2}} q(x,y,z,t^n)\, dz\, dy\, dx, \tag{39}$$

$$\left.\begin{aligned} f_{i+1/2,j,k} &= \frac{1}{\Delta t}\frac{1}{\Delta y}\frac{1}{\Delta z}\int_{y_{j-1/2}}^{y_{j+1/2}}\int_{z_{k-1/2}}^{z_{k+1/2}}\int_{t^n}^{t^{n+1}} f(q(x_{i+1/2},y,z,\tau))\, d\tau\, dz\, dy, \\ g_{i,j+1/2,k} &= \frac{1}{\Delta t}\frac{1}{\Delta x}\frac{1}{\Delta z}\int_{x_{i-1/2}}^{x_{i+1/2}}\int_{z_{k-1/2}}^{z_{k+1/2}}\int_{t^n}^{t^{n+1}} g(q(x,y_{i+1/2},z,\tau))\, d\tau\, dz\, dx, \\ h_{ij,k+1/2} &= \frac{1}{\Delta t}\frac{1}{\Delta x}\frac{1}{\Delta y}\int_{x_{i-1/2}}^{x_{i+1/2}}\int_{y_{j-1/2}}^{y_{j+1/2}}\int_{t^n}^{t^{n+1}} h(q(x,y,z_{i+1/2},\tau))\, d\tau\, dy\, dx, \end{aligned}\right\} \tag{40}$$

$$s_{ij} = \frac{1}{\Delta t}\frac{1}{\Delta x}\frac{1}{\Delta y}\frac{1}{\Delta z}\int_{t^n}^{t^{n+1}}\int_{x_{i-1/2}}^{x_{i+1/2}}\int_{y_{j-1/2}}^{y_{j+1/2}}\int_{z_{k-1/2}}^{z_{k+1/2}} s(x,y,z,t,q)\, dz\, dy\, dx\, dt. \tag{41}$$

The procedure to evaluate the numerical flux in three space dimensions is a straightforward extension of the two-dimensional one. We again concentrate on $f_{i+1/2,jk}$; the expressions for $g_{i,j+1/2,k}$, $h_{ij,k+1/2}$ are obtained in an entirely analogous manner. First we discretize the spatial integrals over the cell faces in (40) using a tensor product of a suitable Gaussian numerical quadrature. The expression for the numerical flux in the x coordinate direction then reads

$$f_{i+1/2,jk} = \sum_{\alpha=1}^{N}\sum_{\beta=1}^{N}\left(\frac{1}{\Delta t}\int_{t^n}^{t^{n+1}} f(q(x_{i+1/2},y_\alpha,z_\beta,\tau))d\tau\right) K_\beta\, K_\alpha, \tag{42}$$

where y_α, z_β are the integration points over the cell face $[x_{i-1/2}, x_{i+1/2}] \times [y_{j-1/2}, y_{j+1/2}]$ and K_α, K_β are the weights. Next we reconstruct the point-wise values of the solution from cell averages to high order of accuracy at the Gaussian integration points $(x_{i+1/2}, y_\alpha, z_\beta)$, including all derivatives up to order $r-1$ for the scheme of the r^{th} order of accuracy. Reconstruction in three space dimensions is a straight-forward generalization of the two-dimensional algorithm and consists of three one-dimensional sweeps [19]. First we perform a one-dimensional WENO sweep in the x direction (normal to the face) and obtain left and right $y-z$ averages of q and its x derivatives. Then we perform the one-dimensional sweep in y direction to obtain z averages of q and its mixed $x-y$ derivatives for Gaussian integration points in y direction. Finally,

we obtain the sought point-wise values by performing the one-dimensional WENO sweep in z direction. See [19] for more details.

After the reconstruction is carried out for each Gaussian integration point (y_α, z_β) at the cell face we pose the generalized Riemann problem (4) in the x-coordinate direction (normal to the cell boundary) and obtain a high order approximation to $q(x_{i+1/2}, y_\alpha, z_\beta, \tau)$. All steps of the solution procedure remain essentially as in the two-dimensional case. First, we write Taylor series expansion in time

$$q(x_{i+1/2}, y_\alpha, z_\beta, \tau) = q(x_{i+1/2}, y_\alpha, z_\beta, 0+) + \sum_{k=1}^{r-1} \left[\partial_t^{(k)} q(x_{i+1/2}, y_\alpha, z_\beta, 0+)\right] \frac{\tau^k}{k!}. \tag{43}$$

The leading term $q(x_{i+1/2}, y_\alpha, z_\beta, 0+)$ is the self-similar solution of the conventional Riemann problem

$$\left.\begin{array}{c} \partial_t q + \partial_x f(q) = 0, \\ q(x,0) = \left\{ \begin{array}{lll} q_L(x_{i+1/2}, y_\alpha, z_\beta) & \text{if} & x < x_{i+1/2}, \\ q_R(x_{i+1/2}, y_\alpha, z_\beta) & \text{if} & x > x_{i+1/2}, \end{array} \right. \end{array}\right\} \tag{44}$$

evaluated at $(x - x_{i+1/2})/t = 0$. Next, we replace all time derivatives by space derivatives using (37) by means of the Cauchy-Kowalewski procedure which will now involve x, y and z derivatives up to order $r-1$. For example, for the inviscid reactive Burgers' equation

$$q_t + \left(\frac{1}{2}q^2\right)_x + \left(\frac{1}{2}q^2\right)_y + \left(\frac{1}{2}q^2\right)_z = Aq \tag{45}$$

the Cauchy-Kowalewski procedure yields the following expressions for time derivatives:

$$\begin{aligned} q_t &= -qq_x - qq_y - qq_z + Aq, \\ q_{tt} &= q_x q q_z + 2q q_x^2 + q^2 q_{xx} + 2q^2 q_{xy} + 2q^2 q_x z + 2q {q_y}^2 + q^2 q_{yy} + 2q^2 q_y z + \\ &\quad 2q q_z^2 + q^2 q_{zz} + A^2 q - 3\, q_x\, Aq + 4\, q_y\, q q_z - 3\, q_z\, Aq + 4\, q_x\, q q_y - 3\, q_y\, Aq, \end{aligned} \tag{46}$$

and so on. The expressions in (46) contain space derivatives of the solution

$$q^{(k_1,k_2,k_3)} = \frac{\partial^{k_1+k_2+k_3}}{\partial x^{k_1} \partial y^{k_2} \partial z^{k_3}} q, \quad q^{(1,0,0)} \equiv q_x, \quad q^{(0,1,0)} \equiv q_y, \quad q^{(0,0,1)} \equiv q_z, \ldots \tag{47}$$

Again, it can be shown that all $q^{(k_1,k_2,k_3)}$ obey inhomogeneous evolution equations, which are obtained by taking spatial derivatives of the governing equation. Then all $q^{(k_1,k_2,k_3)}$ can be computed as Godunov states of the following linear derivative Riemann problems:

$$\begin{array}{c} \partial_t q^{(k_1,k_2,k_3)} + \lambda_{i+1/2,\alpha\beta}\, \partial_x q^{(k_1,k_2,k_3)} = 0, \quad \lambda_{i+1/2,\alpha\beta} = \lambda(q(x_{i+1/2}, y_\alpha, z_\beta, 0+)) \\ q^{(k_1,k_1,k_3)}(x,0) = \left\{ \begin{array}{l} \dfrac{\partial^{k_1+k_2+k_3}}{\partial x^{k_1} \partial y^{k_2} \partial z^{k_3}} q_L(x_{i+1/2}, y_\alpha, z_\beta), \quad x < x_{i+1/2} \\ \dfrac{\partial^{k_1+k_2+k_3}}{\partial x^{k_1} \partial y^{k_2} \partial z^{k_3}} q_R(x_{i+1/2}, y_\alpha, z_\beta), \quad x > x_{i+1/2} \end{array} \right. \end{array} \tag{48}$$

Here

$$\frac{\partial^{k_1+k_2+k_3}}{\partial x^{k_1} \partial y^{k_2} \partial z^{z_3}} q_L(x_{i+1/2}, y_\alpha, z_\beta), \quad \frac{\partial^{k_1+k_2+k_3}}{\partial x^{k_1} \partial y^{k_2} \partial z^{z_3}} q_R(x_{i+1/2}, y_\alpha, z_\beta)$$

are left and right reconstructed point-wise values of derivatives. After solving (48) for $1 \leq k_1+k_2+k_3 \leq r-1$ we substitute $q^{(k_1 k_2 k_3)}$ into the Taylor expansion (43) and form a polynomial $q_{i+1/2,\alpha,\beta}(\tau)$:

$$q_{i+1/2,\alpha,\beta}(\tau) = c_0 + c_1\tau + c_2\tau^2 + \ldots + c_{r-1}\tau^{r-1}, \quad 0 \leq \tau \leq \Delta t, \quad c_i = \text{constant} \tag{49}$$

which approximates the interface state $q(x_{i+1/2}, y_\alpha, z_\beta, \tau)$ at the Gaussian integration point $(x_{i+1/2}, y_\alpha, z_\beta)$ to the r^{th} order of accuracy.

The flux of the **state-expansion** ADER scheme is given by

$$f_{i+1/2,jk} = \sum_{\alpha=1}^{N}\sum_{\beta=1}^{N}\left(\sum_{l=1}^{N} f(q(x_{i+1/2}, y_\alpha, z_\beta, \tau_l))K_l\right) K_\beta\, K_\alpha. \tag{50}$$

For the **flux expansion** ADER schemes we write Taylor time expansion of the physical flux at each point $(x_{i+1/2},\, y_\alpha,\, z_\beta)$

$$f(x_{i+1/2}, y_\alpha, z_\beta, \tau) = f(x_{i+1/2}, y_\alpha, z_\beta, 0+) + \sum_{k=1}^{r-1}\left[\partial_t^{(k)} f(x_{i+1/2}, y_\alpha, z_\beta, 0+)\right]\frac{\tau^k}{k!}. \tag{51}$$

Similar to the two-dimensional case, the leading term $f(x_{i+1/2}, y_\alpha, z_\beta, 0+)$ is computed from (44) using a monotone flux, such as Godunov's first order upwind flux. The remaining higher order time derivatives of the flux in (51) are expressed via time derivatives of the intercell state $q_{i+1/2,\alpha,\beta}(\tau)$. These time derivatives are computed from Taylor expansion (49). The numerical flux is then given by

$$f_{i+1/2,jk} = \sum_{\alpha=1}^{N}\sum_{\beta=1}^{N}\left(f(x_{i+1/2}, y_\alpha, z_\beta, 0+) + \sum_{k=1}^{r-1}\left[\partial_t^{(k)} f(x_{i+1/2}, y_\alpha, z_\beta, 0+)\right]\frac{\Delta t^k}{(k+1)!}\right) K_\alpha K_\beta\,. \tag{52}$$

The computation of the numerical source now involves four-dimensional integration. First we use the tensor-product of the N-point Gaussian rule to discretize the three-dimensional space integral in (41) so that the expression for s_{ijk} reads

$$s_{ijk} = \sum_{\alpha=1}^{N}\sum_{\beta=1}^{N}\sum_{\gamma=1}^{N}\left(\frac{1}{\Delta t}\int_{t^n}^{t^{n+1}} s(x_\alpha, y_\beta, z_\gamma, \tau, q(x_\alpha, y_\beta, z_\gamma, \tau))d\tau\right) K_\gamma K_\beta K_\alpha. \tag{53}$$

Then we reconstruct values and all spatial derivatives, including mixed derivatives, of q at the Gaussian integration point in $x-y-z$ space for the time level t^n. Note that these points are different from flux integration points over cell faces. The reconstruction procedure is entirely analogous to that for the flux evaluation. Next for each Gaussian point $(x_\alpha, y_\beta, z_\gamma)$ we perform the Cauchy-Kowalewski procedure and replace time derivatives by space derivatives. As a result we have high-order approximations to $q(x_\alpha, y_\beta, z_\gamma, \tau)$. Finally, we carry out numerical integration in time using the Gaussian quadrature:

$$s_{ijk} = \sum_{\alpha=1}^{N}\sum_{\beta=1}^{N}\sum_{\gamma=1}^{N}\left(\sum_{l=1}^{N} s(x_\alpha, y_\beta, z_\gamma, \tau, q(x_\alpha, y_\beta, z_\gamma, \tau_l))K_l\right) K_\gamma K_\beta K_\alpha. \tag{54}$$

The solution is advanced by one time step by updating the cell averages of the solution according to the one-step formula (38).

The explicit scheme considered above requires the computation of a time step Δt to be used in the conservative updates (2), (20), (38), such that stability of the numerical method is ensured. One way of choosing Δt is

$$\Delta t = C_{cfl} \times \min_{ijk} \left(\frac{\Delta x}{|\lambda_{ijk}^{n,x}|}, \frac{\Delta y}{|\lambda_{ijk}^{n,y}|}, \frac{\Delta z}{|\lambda_{ijk}^{n,z}|} \right). \tag{55}$$

Here $\lambda_{ijk}^{n,d}$ is the speed of the fastest wave present at time level n travelling in the d direction, with $d = x, y, z$. C_{cfl} is the CFL number and is chosen according to the linear stability condition of the scheme.

In one space dimension linear schemes applied to the linear homogeneous advection equation with constant coefficient have the optimal stability condition $C_{cfl} \leq 1$. [22]. Numerical experiments indicate that the approach has the same stability condition for nonlinear scalar equations and systems as well [17].

The linear stability analysis of ADER schemes in two and three space dimensions is not available yet. Numerical experiments indicate that ADER schemes have a reduced stability condition which in fact coincides with the stability condition of the unsplit Godunov scheme [5] and ENO/WENO schemes [2, 14]. In two space dimensions the stability condition is $0 < C_{cfl} \leq 1/2$ and in three space dimensions the stability condition is $0 < C_{cfl} \leq 1/3$.

When the source term is present it should also be taken into account when choosing the stable time step.

5 Numerical results

In this section we present numerical results of the state-expansion ADER schemes of up to fifth order of accuracy as applied to scalar homogeneous equations. The detailed evaluation of ADER for equations with source terms and the flux-expansion ADER in several space dimensions is the subject of ongoing research. These examples illustrate that the ADER schemes can compute discontinuous solutions without oscillations and at the same time maintain the designed very high order of accuracy in *both time and space* in multiple space dimensions. In all examples for flux integration we use the two-point 4^{th}-order Gaussian rule for third and forth-order ADER schemes and the three-point 6^{th}-order Gaussian rule for the fifth order ADER scheme.

We remark that it seems to have become a popular practice to check the formal order of very high-order schemes by running them with very small Courant numbers or choosing the time step in such a way that the spatial order dominates the computation [1, 3]. This results in exceedingly small time steps and therefore *enormous* computational cost of the scheme. This is especially so in many space dimensions. In practical calculations, however, for hyperbolic equations one uses a *fixed* Courant number which should be as close as possible to the maximum allowed value given in the previous section. In this paper our goal is to compare the performance of different methods in a realistic setup. Thus we use a fixed Courant number $C_{cfl} = 0.45$ in two space dimensions and $C_{cfl} = 0.27$ in three space dimensions in all numerical examples.

Table 1: Convergence study for the 2D linear advection equation with variable coefficients (56) with initial condition (58) and $\delta = 1$ at output time $t = 4$. CFL= 0.45 for all schemes. N is the number of cells in each coordinate direction.

Method	N	L_∞ error	L_∞ order	L_1 error	L_1 order
ADER3	50	2.92×10^{-1}		6.53×10^{-1}	
	100	7.56×10^{-2}	1.95	1.16×10^{-1}	2.49
	200	9.27×10^{-3}	3.03	1.12×10^{-2}	3.38
	400	7.47×10^{-4}	3.63	6.65×10^{-4}	4.07
ADER4	50	2.04×10^{-1}		3.67×10^{-1}	
	100	2.95×10^{-2}	2.79	3.95×10^{-2}	3.22
	200	2.63×10^{-3}	3.49	2.51×10^{-3}	3.98
	400	3.22×10^{-5}	6.35	2.57×10^{-5}	6.61
ADER5	50	1.36×10^{-1}		2.84×10^{-1}	
	100	2.10×10^{-2}	2.69	3.06×10^{-2}	3.21
	200	1.26×10^{-3}	4.06	9.47×10^{-4}	5.01
	400	2.08×10^{-5}	5.92	1.70×10^{-5}	5.80

5.1 The kinematic frontogenesis problem

This test problem [6] is important in meteorology where it models a real effect taking place in the Earth atmosphere. From the numerical point of view it tests the ability of the schemes to handle moving discontinuities in two space dimensions. We remark that a number of advection schemes has been reported to fail for this test problem, especially those using dimensional splitting.

We solve the two-dimensional linear equation with variable coefficients

$$q_t + \left(u(x,y)q\right)_x + \left(v(x,y)q\right)_y = 0, \tag{56}$$

where (u, v) is a steady divergence-free velocity field:

$$\begin{gathered} u = -y\,\omega(r), \quad v = x\,\omega(r), \quad \omega(r) = \frac{1}{r}\,U_T(r), \quad r^2 = x^2 + y^2, \\ U_T(r) = U_{max}\,\mathrm{sech}^2(r)\tanh(r), \quad U_{max} = 2.5980762. \end{gathered} \tag{57}$$

The initial distribution of $q(x, y, t)$, defined on a square domain $[-5, 5] \times [-5, 5]$, is assumed to be one-dimensional

$$q(x, y, 0) = q_0(y) = \tanh\left(\frac{y}{\delta}\right), \tag{58}$$

where δ expresses the characteristic width of the front zone. The exact solution is then given

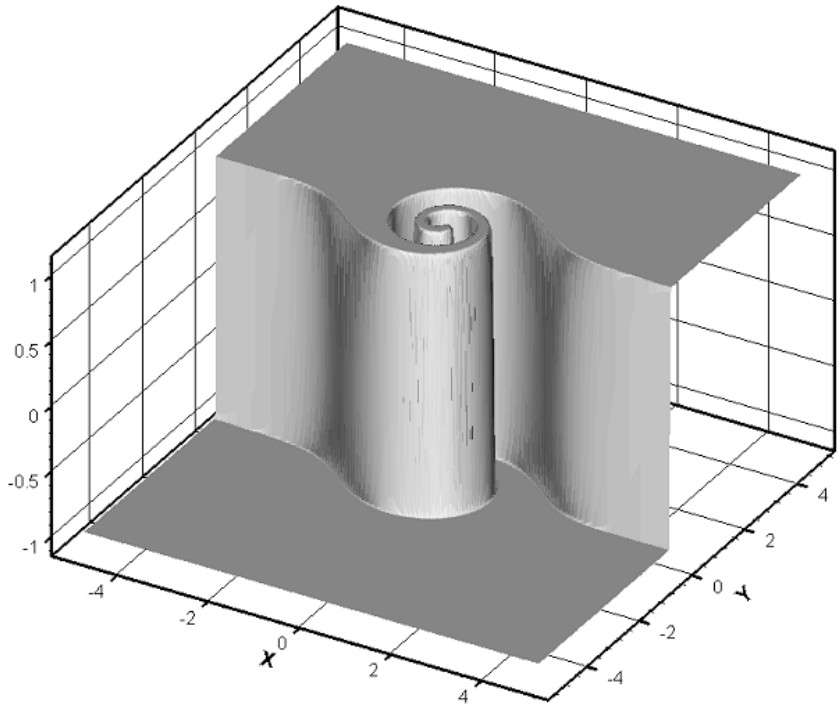

Figure 1: Solution of the two-dimensional linear advection equation (56) with the initial condition (58) and $\delta = 10^{-6}$ at output time $t = 4$ and CFL= 0.45. Method: the ADER5 scheme. Mesh of 401×401 cells is used.

by [6]

$$q(x, y, t) = q_0(y\cos(\omega t) - x\sin(\omega t)) \tag{59}$$

and represents a rotation of the initial distribution around the origin with variable angular velocity $\omega(r)$. We note that as time evolves the solution will eventually develop scales which will be beyond the resolution of the computational mesh.

We first consider a smooth solution with $\delta = 1$. Table 1 shows a convergence study for cell averages at the output time $t = 4$. Obviously, all schemes achieve the design order of accuracy. The size of the error decreases as the formal order of the scheme increases. Moreover, the forth and fifth order schemes show sixth order of accuracy on fine meshes. We would like to stress the fact that such high orders of accuracy are achieved for a *fixed* Courant number.

Next we compute the numerical solution which corresponds to a discontinuous initial distribution with $\delta = 10^{-6}$. At the given output time the initial discontinuity has been rotated several times and the solution represents a discontinuous rolling surface.

Figs. 1 – 2 depict, respectively, a three-dimensional plot and contour plot of the numerical solution obtained by the fifth order ADER scheme. We observe that the numerical solution is essentially non-oscillatory with sharp resolution of all discontinuities. All parts of the discontinuous rolling surface have been captured well. Further illustration is provided by Figures 3 – 5, which show one-dimensional cuts along the y axis for $-3 \le y \le 3$; results of the third, forth and fifth order schemes on the meshes of 201×201 cells and 401×401 cells are shown. In all figures the solid line corresponds to point-wise values of the exact solution whereas symbols correspond to the numerical solution (cell averages). Clearly all schemes capture all features

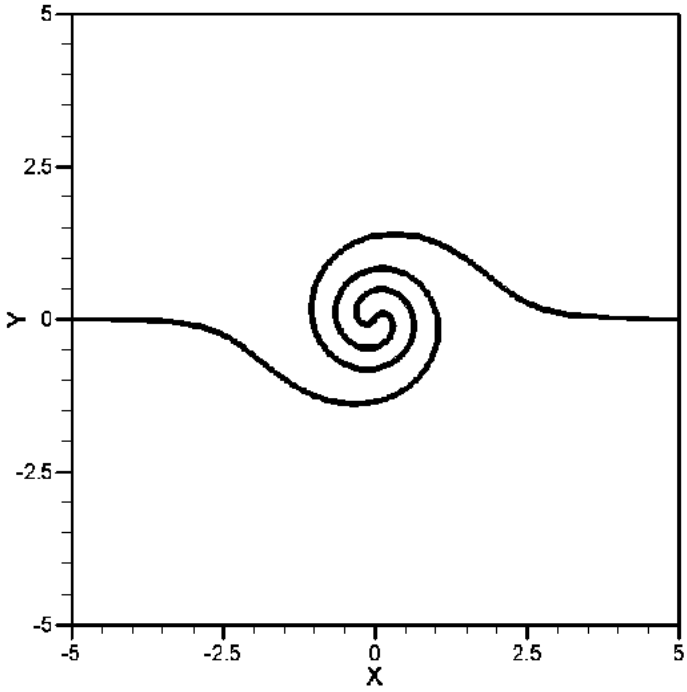

Figure 2: Contours of the solution of the two-dimensional linear advection equation (56) with the initial condition (58) and $\delta = 10^{-6}$ at output time $t = 4$ and CFL= 0.45. Method: the ADER5 scheme. Mesh of 401×401 cells is used. See also Fig. 1.

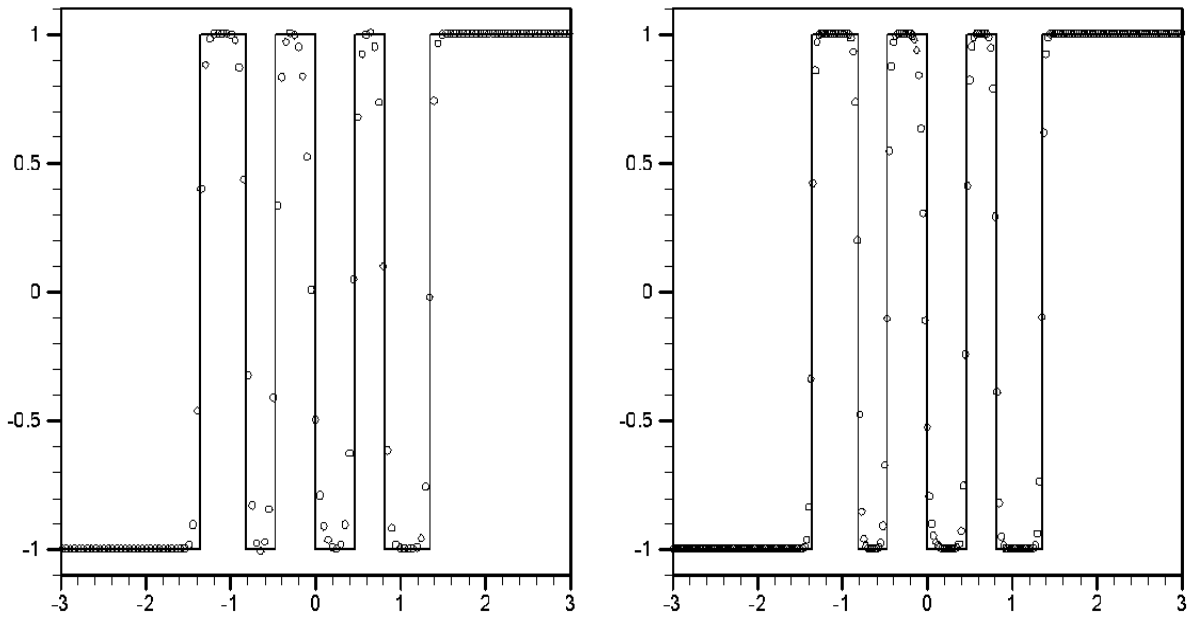

Figure 3: One-dimensional cuts along the y axis for the two-dimensional linear advection equation (56) with the initial condition (58) and $\delta = 10^{-6}$ at output time $t = 4$ and CFL= 0.45. Solid line shows point-wise values of the exact solution and symbols show cell averages computed by the ADER3 scheme. The meshes of 201×201 cells (left) and 401×401 cells (right) are used.

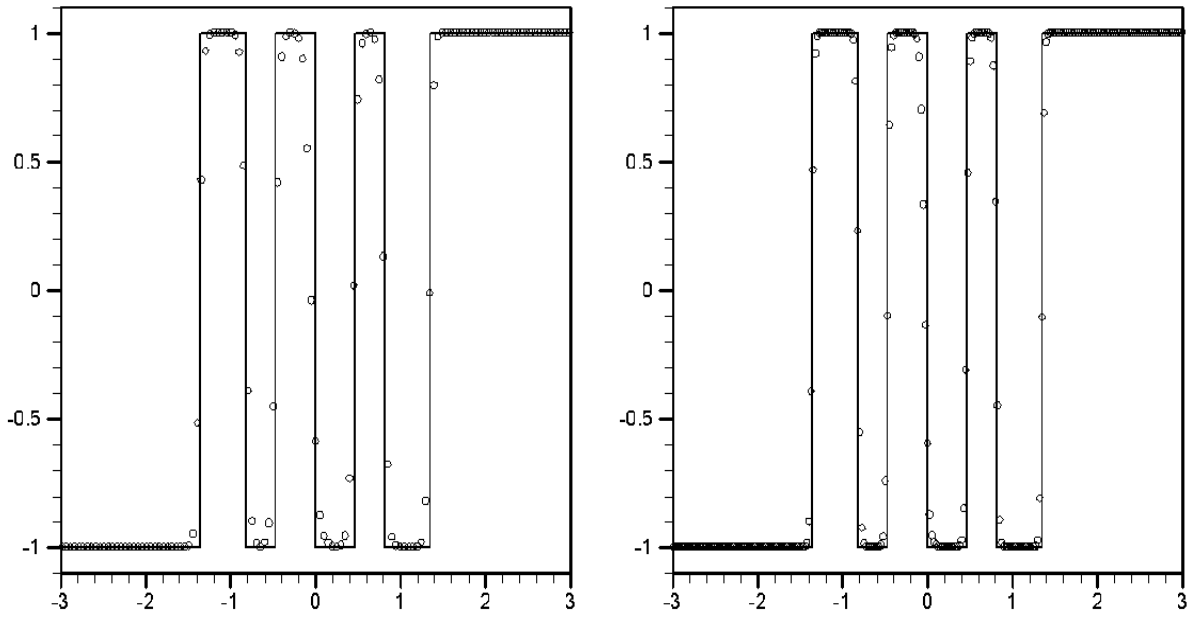

Figure 4: One-dimensional cuts along the y axis for the two-dimensional linear advection equation (56) with the initial condition (58) and $\delta = 10^{-6}$ at output time $t = 4$ and CFL= 0.45. Solid line shows point-wise values of the exact solution and symbols show cell averages computed by the ADER4 scheme. The meshes of 201×201 cells (left) and 401×401 cells (right) are used.

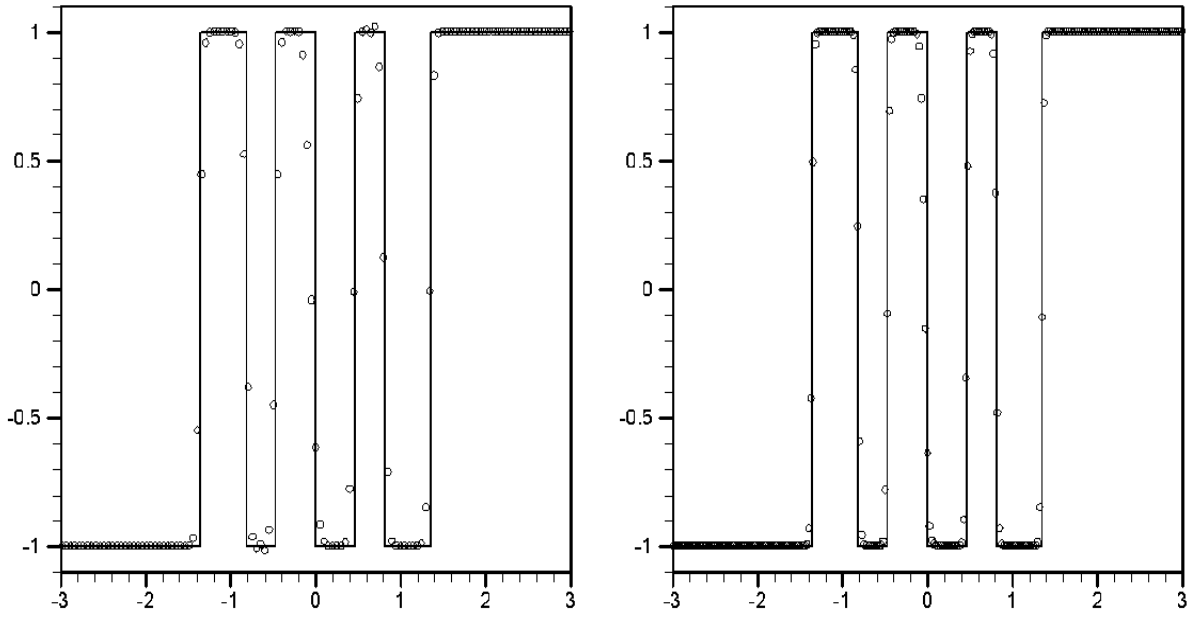

Figure 5: One-dimensionals cut along the y axis for the two-dimensional linear advection equation (56) with the initial condition (58) and $\delta = 10^{-6}$ at output time $t = 4$ and CFL= 0.45. Solid line shows point-wise values of the exact solution and symbols show cell averages computed by the ADER5 scheme. The meshes of 201×201 cells (left) and 401×401 cells (right) are used.

Table 2: Convergence study for the 3D inviscid Burgers' equation (60) with initial condition (61) at output time $t = 0.05$. CFL= 0.27 for all schemes. N is the number of cells in each coordinate direction.

Method	N	L_∞ error	L_∞ order	L_1 error	L_1 order
ADER3	5	1.84×10^{-2}		3.34×10^{-2}	
	10	2.05×10^{-3}	3.17	3.47×10^{-3}	3.27
	20	3.89×10^{-4}	2.39	2.09×10^{-4}	4.05
	40	4.85×10^{-5}	3.00	1.74×10^{-5}	3.59
	80	6.99×10^{-6}	2.79	2.18×10^{-6}	3.00
ADER4	5	1.90×10^{-2}		2.21×10^{-2}	
	10	1.07×10^{-3}	4.14	5.82×10^{-4}	5.25
	20	6.64×10^{-5}	4.01	2.25×10^{-5}	4.70
	40	5.10×10^{-6}	3.70	1.27×10^{-6}	4.15
	80	3.07×10^{-7}	4.05	8.27×10^{-8}	3.94
ADER5	5	4.77×10^{-3}		7.96×10^{-3}	
	10	2.42×10^{-4}	4.30	1.17×10^{-4}	6.09
	20	1.07×10^{-5}	4.50	3.50×10^{-6}	5.06
	40	2.75×10^{-7}	5.28	1.06×10^{-7}	5.04
	80	8.79×10^{-9}	4.97	3.95×10^{-9}	4.75

correctly. The resolution of the discontinuities improves as the formal order of accuracy of the scheme increases, which is more clearly shown in the finer mesh results. We observe slight oscillations in the result of the ADER5 scheme for the internal steps in the y cut of $q(x, y, t)$. These oscillations are due to the fact that the essentially non-oscillatory reconstruction cannot find a smooth stencil on this coarse mesh. Indeed, there are only four cells between discontinuities in the middle, whereas the forth order polynomials used in the reconstruction need at least five cells. When the mesh is refined further the oscillations vanish rapidly.

5.2 The three-dimensional inviscid Burgers' equation

We solve the three-dimensional inviscid Burgers' equation

$$q_t + \left(\frac{1}{2}q^2\right)_x + \left(\frac{1}{2}q^2\right)_y + \left(\frac{1}{2}q^2\right)_z = 0 \tag{60}$$

with the following initial condition defined on $[-1, 1] \times [-1, 1] \times [-1, 1]$:

$$q(x, y, z, 0) = q_0(x, y, z) = 0.25 + \sin(\pi x)\sin(\pi y)\sin(\pi z) \tag{61}$$

and periodic boundary conditions. For this test problem the exact solution is obtained by solving numerically the relation $q = q_0(x - qt, y - qt, z - qt)$ for a given point (x, y, z) and time t. The cell averages of the exact solution at the output time are computed using the 8^{th}-order Gaussian rule.

Table 2 shows the errors at the output time $t = 0.05$, when the solution is still smooth. We observe that all ADER schemes reach the design r^{th} order of accuracy in both norms. Moreover, the error decreases by an order of magnitude when the formal order of accuracy increases. As expected, the fifth order scheme is the most accurate scheme. Again, we would like to stress the fact that such high orders of accuracy are achieved for a *fixed* Courant number.

6 Conclusions

The design of nonlinear ADER schemes of upto fifth order in both time and space as applied to scalar linear and nonlinear advection-reaction equations was presented. The numerical results for the linear advection equation with variable coefficients and for the inviscid Burgers' equation suggest that for smooth solutions the schemes retain the designed order of accuracy for realistic CFL numbers. When the solution is discontinuous the schemes produce essentially non-oscillatory results and sharp resolution of discontinuities. The extension to nonlinear hyperbolic systems in 2D and 3D is the subject of ongoing research.

References

[1] Balsara D.S. and Shu C.W. (2000). Monotonicity preserving weighted essentially non-oscillatory schemes with increasingly high order of accuracy. *J. Comput. Phys*, **160**, pp. 405-452.

[2] Casper J. and Atkins H. (1993). A finite-volume high order ENO scheme for two dimensional hyperbolic systems. *J. Comput. Phys.*, **106**, pp. 62-76.

[3] Cockburn B. and Shu C.-W. (2001). Runge-Kutta Discontinuous Galerkin methods for convection-dominated problems. *J. Sci. Comput.*, **16**, pp. 173-261.

[4] Colella P. (1990). Multidimensional upwind methods for hyperbolic conservation laws. *J. Comput. Phys.*, **87**, pp. 171-200.

[5] Godunov SK. (1959). A finite difference method for the computation of discontinuous solutions of the equations of fluid dynamics. *Mat. Sbornik*, **47**, pp. 357-393.

[6] Davies-Jones R. (1985). Comments on 'A kinematic analysis of frontogenesis associated with a non-divergent vortex'. *J. Atm. Sci.*, **42**, pp. 2073-2075.

[7] Jiang G.S. and Shu C.W. (1996). Efficient implementation of weighted ENO schemes. *J. Comput. Phys.*, **126**, pp. 202–212.

[8] Harten A, Engquist B, Osher S and Chakravarthy S.R. (1987). Uniformly high order accurate essentially non-oscillatory schemes III. *J. Comput. Phys.*, **71**, pp. 231-303.

[9] Hu C. and Shu C.-W. (1999). Weighted essentially non-oscillatory schemes on triangular meshes. *J. Comput. Phys.*, **150**, pp. 97-127.

[10] Kolgan N.E. (1972). Application of the minimum-derivative principle in the construction of finite-difference schemes for numerical analysis of discontinuous solutions in gas dynamics. *Uchenye Zapiski TsaGI* [Sci. Notes of Central Inst. of Aerodynamics], **3**, No. 6, pp. 68-77 (in Russian).

[11] Kolgan N.E. (1975). Finite-difference schemes for computation of three dimensional solutions of gas dynamics and calculation of a flow over a body under an angle of attack. *Uchenye Zapiski TsaGI* [Sci. Notes of Central Inst. of Aerodynamics], **6**, No. 2, pp. 1-6 (in Russian).

[12] Liu X.D. and Osher S. and Chan T. (1994). Weighted essentially non-oscillatory schemes. *J. Comput. Phys.*, **115**, pp. 200-212.

[13] Schwartzkopff T., Munz C.D. and Toro E.F. (2002) ADER-2D: a high-order approach for linear hyperbolic systems in 2D. *J. Sci. Comput.*, **17**, pp. 231-240.

[14] Shi J., Hu C. and Shu C.-W. (2002). A technique for treating negative weights in WENO schemes. *J. Comput. Phys.*, **175**, pp. 108-127.

[15] Tilaeva N.N. (1986). A generalization of the modified Godunov scheme to arbitrary unstructured meshes. *Uchenye Zapiski TsaGI* [Sci. Notes of Central Inst. of Aerodynamics], **17**, pp. 18-26, 1986 (in Russian)

[16] Takakura Y and Toro E.F. (2002). Arbitrarily accurate non-oscillatory schemes for a nonlinear conservation law. *CFD Journal*, **11**, N. 1, pp. 7-18.

[17] Titarev V.A. and Toro E.F. (2002). ADER: Arbitrary High Order Godunov Approach. *J. Sci. Comput.*, **17**, pp. 609-618.

[18] Titarev V.A. and Toro E.F. (2003) High order ADER schemes for the scalar advection-reaction-diffusion equations, *CFD Journal*, **12**, N. 1, pp. 1-6.

[19] Titarev V.A. and Toro E.F. (2003). Finite-volume WENO schemes for three-dimensional conservation laws. Preprint NI03057-NPA. Isaac Newton Institute for Mathematical Sciences, University of Cambridge, UK. - 2003. - 33 P., submitted.

[20] Toro E.F. (1989). A weighted average flux method for hyperbolic conservation laws. *Proc. Roy. Soc. London*, A 423, pp. 401-418.

[21] Toro E.F. (1999). *Riemann Solvers and Numerical Methods for Fluid Dynamics*. Second Edition, Springer-Verlag.

[22] Toro E.F., Millington R.C. and Nejad L.A.M. (2001). Towards very high order Godunov schemes. In: E. F. Toro (Editor). Godunov Methods. Theory and Applications, Edited Review, Kluwer/Plenum Academic Publishers, pp. 907-940, 2001.

[23] Toro E.F. and Titarev V.A. (2002). Solution of the Generalised Riemann Problem for Advection-Reaction Equations. *Proc. Roy. Soc. London*, 458(2018), pp. 271-281.

[24] Toro E.F and Titarev V.A. (2003). TVD Fluxes for the High-Order ADER Schemes, Preprint NI03011-NPA. Isaac Newton Institute for Mathematical Sciences, University of Cambridge, UK. - 2003. – 37 P., submitted

[25] van Leer B. (1973). Towards the ultimate conservative difference scheme I: the quest for monotonicity. *Lecture Notes in Physics* **18**, pp. 163-168.

[26] van Leer B. (1979). Towards the ultimate conservative difference scheme V: a second order sequel to Godunov' method. *J. Comput. Phys.* **32**, pp. 101-136.